DTU Library

Nonlinear analysis of combustion instabilities in a confined multipoint injection configuration

Jomaas, Grunde

Publication date:
2009

Document Version
Early version, also known as pre-print

Nonlinear analysis of combustion instabilities in a confined multipoint injection configuration

F. Boudy[1,*], G. Jomaas[2], D. Durox[1], T. Schuller[1], S. Candel[1]
[1]*Ecole Centrale Paris, EM2C Laboratory, CNRS, 92295 Châtenay-Malabry, France*
[2]*Technical University of Denmark, Dept. of Civil Engineering, 2800 Kgs. Lyngby, Denmark*
*frederic.boudy@em2c.ecp.fr

Abstract

Self-sustained combustion instabilities in a premixed multipoint injection configuration are investigated and it is shown that a nonlinear analysis based on the flame describing function (FDF) is necessary to properly describe the experimentally observed effect that the unsteady combustion process has on the resonant frequencies. The setup features a feeding manifold of variable length, a set of conical flames anchored on a perforated plate and a flame confinement tube. Unstable regimes are characterized at the limit cycle using fluctuating pressure and velocity measurements inside the feeding manifold. Light emission from OH* radicals formed in the flame is recorded to obtain estimates of the heat release rate oscillations. The nonlinear stability analysis yields predictions of the limit cycle oscillations that can be directly compared with the experimental data.

1. Experimental setup

A schematic view of the combustor is given in figure 1. The burner is fed by a methane-air mixture through a piston that is also used to vary the length, L_1, of the feeding manifold. Air and methane are separately injected at the piston base and the equivalence ratio is fixed to 0.90 with a total mass flow rate of 3.65 10^{-3} kg s^{-1}. A perforated plate is then used to anchor a set of conical laminar flames (an instantaneous view of the flame motion is sketched in Figure 1). The burner assembly also features a quartz tube of length L_2 = 0.10 m and diameter D_2 = 0.13 m to confine the flames.

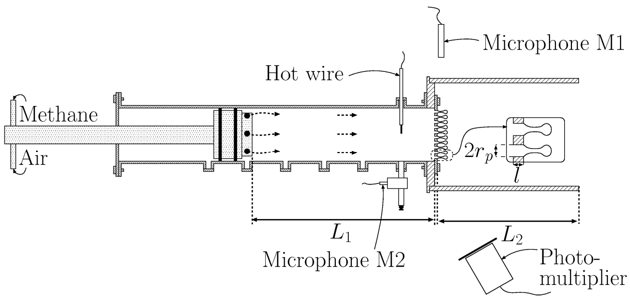

Figure 1 Schematic of the burner configuration and the diagnostics.

The perforated plate of thickness l=3 mm and diameter $2R$=70 mm comprises N=189 holes of diameter $2r_p$=3 mm set on a 4.4 mm square mesh, corresponding to a porosity $P=N\pi r_p^2/\pi R^2=0.35$. Sound pressure signals are measured by microphones M1 outside the setup and M2 located on a waveguide inside the feeding manifold 3 cm upstream of the plate. A hot-wire that measures the local flow velocity is located adjacent to M2. Finally, a photomultiplier equipped with an OH* filter is viewing the flames from outside the quartz tube.

2. Experimental results

This setup was used to characterize the observed unstable modes at limit cycles by simultaneously recording oscillations of OH*, the sound pressure and the velocity as the length of the resonant cavity L_1 is swept from 0.10 m to 0.54 m with steps of 0.01 m. The peak oscillation frequency and the sound level measured by M2 are plotted as function of L_1 in Figure 2 (circles).

3. Burner acoustics and theoretical modelling

The burner acoustics are determined both without and with inclusion of the flame response. In the absence of combustion, one may develop a standard acoustic analysis by only considering longitudinal waves and assuming uniform temperatures T_1=293K and T_2=1800K inside the manifold and the flame tube, respectively. Discarding the role of the perforated plate of large porosity, one obtains the following dispersion relation:

$$\mathcal{H}(\omega) = \frac{\rho_2 c_2}{\rho_1 c_1} \cdot \frac{S_1}{S_2} \sin\left(\frac{\omega L_1}{c_1}\right) \sin\left(\frac{\omega L_2}{c_2}\right) - \cos\left(\frac{\omega L_1}{c_1}\right) \cos\left(\frac{\omega L_2}{c_2}\right) \quad (1)$$

Here S_1 and S_2 respectively stand for the feeding manifold section and the confinement section. c_1 and c_2 represent the speed of sound in each section. Roots of this relation define the set of longitudinal acoustic resonant angular frequencies $\omega=2\pi f$ of the system. Results for these frequencies are plotted in Figure 2(a) (lines) and do not perfectly match the peak oscillation frequencies determined experimentally (circles). This clearly indicates that the observed resonant frequencies are modified by the unsteady combustion process. Thus, the linear analysis cannot be used to determine oscillation levels. However, these two issues can be resolved by including information on the nonlinear flame dynamics in the frequency domain analysis. The methodology employs the FDF framework devised previously [1,2] where the flame response to incoming perturbations is characterized for increasing levels in forced flows configurations. This yields a set of flame transfer functions (Figure 2(b)) designated as the flame describing function (FDF) that can be used to analyze the evolution of the growth rates of perturbations $a' = |a'| \exp(-i\omega t)$ where $\omega = \omega_r + i\omega_i$. In the last expression ω_r is the angular frequency $2\pi f$ and ω_i is the growth rate.

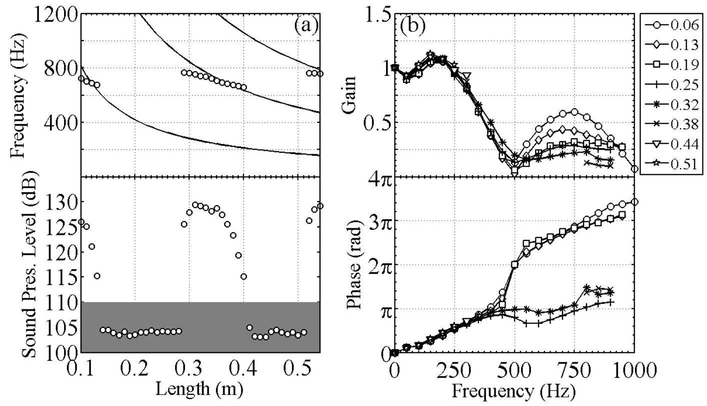

Figure 2 (a) Resonant frequencies and sound pressure level (SPL) of M2 for different length of the feeding manifold (L_1). Confinement L_1=0.10 m. Theoretical frequencies (lines) and measurements (symbols). The shaded gray area corresponds to the overall SPL range measured without combustion.
(b) Experimental flame transfer function for eight values of the normalized driving velocity, u_{rms}/U_{bulk}.

For positive growth rates ω_i perturbations grow whereas they decay for negative values. A previous study of an unconfined configuration provided a good match between predictions and experimental data [1]. The methodology was then extended to take into account effect of flames confinement yielding the following dispersion relation [2]:

$$\begin{aligned}\mathcal{H}(\omega) = {} & \cos\left(\frac{\omega L_1}{c_1}\right)\cos\left(\frac{\omega L_2}{c_2}\right) - \frac{\omega \cdot l}{P \cdot c_1}\left(1 + \frac{l_v}{r_p}(1+i)\right)\sin\left(\frac{\omega L_1}{c_1}\right)\cos\left(\frac{\omega L_2}{c_2}\right) \\ & - \frac{\rho_2 c_2}{\rho_1 c_1} \cdot \frac{S_1}{S_2}\left(1 + \left(\frac{T_2}{T_1} - 1\right) G e^{i\varphi}\right)\sin\left(\frac{\omega L_1}{c_1}\right)\sin\left(\frac{\omega L_2}{c_2}\right)\end{aligned} \quad (2)$$

Here $l_v = (2v/\omega)^{1/2}$ is the viscous acoustic boundary layer thickness and v the kinematic viscosity. Predictions are compared with experimental data in the present study. Combustion dynamics is included through the FDF (Figure 2(b)) in the form of a gain, G, and phase, φ, which shows dependence on the amplitude of the incident fluctuations. The roots of equation (2) are determined numerically for a set of amplitudes of incident perturbations. This process yields frequencies and growth rates that depend on the amplitude. Limit cycle oscillations are obtained when the growth rate equals the damping in the system. This yields an amplitude and a frequency of oscillation that can be directly compared with experimental measurements.

References

[1] N. Noiray, D. Durox, T. Schuller, S. Candel, A unified framework for nonlinear combustion instability analysis based on the flame describing function, *J. Fluid Mech.* 615 (2008) 139-167.

[2] N. Noiray, D. Durox, T. Schuller, S. Candel, A method for estimating the noise level of unstable combustion based on the flame describing function, *Int. J. Aeroacoustics* 8 (2009) 157-176.